Numerical Arts in the Simulation of Star Formation

Masayoshi Kiguchi

RIST, Kinki University

3-4-1 Kowakae, Higashi-Osaka, Osaka, Japan

Abstract

We summarize the numerical technique used in the simulation of the gravitational collapse of the interstellar gas. The dynamical range of 10^{18} in density can be treated using personal computer.

keywords: star formation, gas dynamics, numerical simulation

1 Introduction

We have long time continued the pursuit of the problem of star formation by simulating the gravitational collapse in the interstellar gas[?]. The problem is the following: The isothermal interstellar gas of $10\,\mathrm{K}$ with small angular momentum, with the mass $\simeq 1\,\mathrm{M}$. is in gravitational equilibrium in the radius $\simeq 10^4\,\mathrm{AU}$. When the small density perturbation is given, the gas begins the gravitational collapse. In the final stage of the collapse, what core is formed?

Using personal computer, we have succeeded to calculate the evolution process, which begins the collapse at the density $\rho \simeq 10^{-19}\,\mathrm{g\,cm^{-3}}$, makes the first core and brings about the second collapse and finally bounces at $\rho \simeq 10^{-1}\,\mathrm{g\,cm^{-3}}$.

In this paper, we summarize the calculation techniques used in this simulation.

2 Numerical method

2.1 Basic Equation

The equations which describe the collapse of interstellar gas are the equation of continuity,

$$\frac{\partial \rho}{\partial t} = -\frac{\partial}{\partial x_k}(\rho v_k)$$

the Euler equation

$$\frac{\partial \rho v_i}{\partial t} = -\frac{\partial}{\partial x_k}(\rho v_i v_k + p\delta_{ik}) - \rho\frac{\partial \phi}{\partial x_i}$$

and the energy equation

$$\frac{\partial}{\partial t}(\frac{1}{2}\rho v^2 + \rho\epsilon) = -\frac{\partial}{\partial x_k}(\rho v_i(\frac{1}{2}v^2 + w)) - \rho v_i\frac{\partial \phi}{\partial x_i}$$

where

$$\epsilon = \frac{p}{\rho(\gamma - 1)}$$

is the internal energy density per volume, γ is the adiabatic exponent, and

$$w = \epsilon + \frac{p}{\rho}$$

is the enthalpy density. As the boundary condition, we adopt the solid wall condition.

The gravitational potential ϕ is given by the Poisson equation

$$\Delta\phi = 4\pi G\rho.$$

The boundary value of the gravitational potential is the value of the spherical potential for which total mass in the simulation box is concentrated to the center point.

2.2 Nested grids method

In order to attain sufficient resolutions, we use the nested grids system. The i-th level grids system consists of $2^n \times 2^n \times 2^n - 2^{n-1} \times 2^{n-1} \times 2^{n-1}$ grid cells. The minus term shows that the central part of the grids system is removed and replaced finer grids system. The $(i + 1)$-th level grids system is implanted in the central $2^{n-1} \times 2^{n-1} \times 2^{n-1}$ grids of i-th level grids cells and consists of $2^n \times 2^n \times 2^n - 2^{n-1} \times 2^{n-1} \times 2^{n-1}$

grids cell. The finest level grids system consists $2^n \times 2^n \times 2^n$ grid cells.

As we use the explicit method for the time evolution, the time step widths are restricted by the Courant condition. The reason that we can trace the time evolution in spite of the extreme fine resolutions is that the step width for each nested level is different. If we let the finest nested level f-th level, calculation proceeds as follows: First, in the f-th level grids system, we follow the time evolution with the time step width dt_1 and dt_2. The step width is chosen sufficiently small that the Courant condition is satisfied and the density variation in one step is sufficiently small. Next, we follow the time evolution in $(f-1)$-level grids system with the step width $dt_1 + dt_2$. Next, we follow the evolution for f-level grids system with the step width $dt_3 + dt_4$, and next we follow the evolution for $(f-1)$-level grids system with time step $dt_3 + dt_4$. Then, we proceed to the time evolution for the $(f-2)$-level grids system with time step $dt_1 + dt_2 + dt_3 + dt_4, \cdots$.

If the Courant condition is violated in the intermediate level, we must repeat the calculation, so that we must make dt's sufficiently small.

In order to calculate the flux through the surface of the grids cell which touches the outermost surface of the i-th level, we have to estimate the quantities in the neighbouring cell which lies in the $(i-1)$-th grids system. We estimate this quantities by the interpolation on the line which pass through the vertex of the cell. The scheme of the interpolation is shown in Figure 1. The flux through the surface of i-th level cell which touches the innermost surface of the i-level grids system is determined from the flux through the surface of $(i+1)$-level gird cell to keep the conservation law.
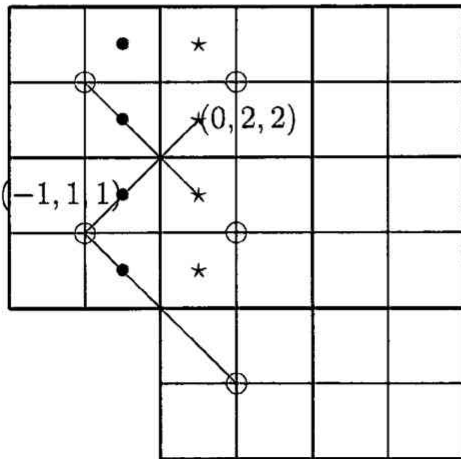

Figure 1: The quantity at • in a virtual cell is interpolated from the quantity at ⋆ in the fine cell

and the quantity at ⊕ in the coarse cell.

2.3 Gravity

We calculate gravitational potential from the coarsest grids system to the finest grids. We calculate the i-th level potential, then find the boundary value of the potential for $(i+1)$-th level, and using this boundary condition we calculate the $(i+1)$-th level gravitation potential. The density distribution in the inner part of coarser grids system is obtained from the finer grids using the reduction procedure which is adjoint to the interpolation procedure.

As the Poisson equation is a linear equation, the superposition principle holds. We solve the Poisson equation as a Dirichlet problem with zero boundary and also solve the Laplace equation with given boundary values. The solution of the Poisson equation with given boundary values is the sum of these two solutions.

The discrete Laplace operator

$$\frac{\frac{f_{i+1,j,k}-f_{i,j,k}}{h} - \frac{f_{i,j,k}-f_{i-1,j,k}}{h}}{h}$$
$$+ \frac{\frac{f_{i,j+1,k}-f_{i,j,k}}{h} - \frac{f_{i,j,k}-f_{i,j-1,k}}{h}}{h}$$
$$+ \frac{\frac{f_{i,j,k+1}-f_{i,j,k}}{h} - \frac{f_{i,j,k}-f_{i,j,k-1}}{h}}{h}$$

is transferred to a simple product operator using trigonometric addition theorem in Fourier transferred space, the solution of the Dirichlet problem in discrete space is fast and stably obtained by the FFT method.

The bothersome point is there in solving the Laplace equation. The solution in two dimensional Laplace equation can be expressed in terms of boundary values in Fourier space. In this case, however, numerical error is large. In the three dimensional case, numerical error exceeds a tolerance level. Therefore, we use the linear multigrid method[?], which makes the numerical solution converge using the prolongation and the reduction procedure. The prolongation is carried out by 8-points linear interpolation, and the reduction operator is selected to be adjoint to the prolongation operator. As the numerical values of the solution for the Laplace equation is between the variation in the boundary values, convergence to the solution is secure and fast.

When we once have used the multigrid method for Poisson equation with given boundary values, we

have faced experience that there are cases convergence was not sufficient and it made the calculation unstable.

2.4 Flux

To solve the conservation equation

$$\frac{\partial f}{\partial t} + \text{div}(\vec{g}) = 0,$$

we have to calculate the flux through the surface of each grid cell. we assume that the physical quantity is constant in each grid cell and is discontinuous at the surface of the cell. We solve approximately the time evolution of the discontinuity, that is, solve the Riemann problem, and estimate the Godunov flux.

In the Riemann problem, the region between nonlinear wave is called star region. The solution procedure to solve the Riemann problem is splitted into three sub-problems:

1. To find star values

$$p_*, u_*, \rho_{*L}, \rho_{*R},$$

where p is the pressure, u is the normal component of the velocity, ρ is the density, and L is left, R is right.

2. To find the solution for tangential velocity v, w throughout the wave structure.

3. To find the solution for ρ and p inside sonic rarefaction.

In solving Riemann problem, we make a large approximation. For the approximate Riemann solver, We use the P(physical)-ordering Osher scheme[?] with the numerical stability in view. In P-ordering Osher scheme, one assumes a-prior that the type of solution for the Riemann problem has a nonlinear two rarefaction wave type. In O(original)-ordering scheme, the type was assumed a-priory to be a two shock type.

P-ordering scheme can treat exactly rarefaction case and gives the correct condition to appear the vacuum region. P-ordering is robust for the case of strong shock and gives good approximate Godunov flux. O-ordering scheme is broken for strong shock but P-ordering withstand for this case.

$u_1 - u_0 \gg 0$ means strong rarefaction, and $u_1 - u_0 \ll 0$ means strong shock. When

$$u_1 - u_0 > \frac{2}{\gamma - 1}(c_{s0} + c_{s1}),$$

where c_s is the sound velocity and γ is the adiabatic exponent, vacuum appears and the calculation breaks down. In this case, we have used the complete upwind scheme.

2.5 Heat

We do not solve the radiative transfer yet. Instead, we have used the barotropic equation of state which is obtained from the simulation of spherical collapse:

- For the case $\rho < \rho_1 = 10^{-16}\,\text{g cm}^{-3}$, $p = \frac{k\rho T}{\mu m_u}$, $T = 10\,\text{K}$, where m_u is the atomic mass units, k the Boltzmann constant, μ the mean molecular weight.

- For the case $\rho_1 < \rho < \rho_2 = 10^{-11}\,\text{g cm}^{-3}$, $p = p_1 \exp[(1 + \frac{\frac{\gamma-1}{3}(\log\frac{\rho}{\rho_1})^2}{(\log\frac{\rho_2}{\rho_1})^2})\log\frac{\rho}{\rho_1}]$, where $p_1 = \frac{k\rho_1 T}{\mu m_u}$,

- For the case $\rho_2 < \rho < \rho_3 = 8.5 \times 10^{-8}\,\text{g cm}^{-3}$, $p = p_2(\frac{\rho}{\rho_2})^\gamma$, where $p_2 = p_1\exp[\frac{\gamma+2}{3}\log\frac{\rho_2}{\rho_1}] = p_1(\frac{\rho_2}{\rho_1})^{\frac{\gamma+2}{3}}$,

- For the case $\rho_3 < \rho < \rho_4 = 10^{-2}\,\text{g cm}^{-3}$, $p = p_3(\frac{\rho}{\rho_3})^{1.18}$, where $p_3 = p_2(\frac{\rho_3}{\rho_2})^\gamma$

- For the case $\rho_4 < \rho$, $p = p_4(\frac{\rho}{\rho_4})^{5/3}$, where $p_4 = p_3(\frac{\rho_4}{\rho_3})^{1.18}$.

When $\rho_3 < \rho < \rho_4$, the gas consists of molecular hydrogen, atomic hydrogen and Helium atom. The adiabatic exponent in this range is given by

$$\gamma = \frac{((k*X + Y/4.)*5./2. + (1-k)/2.*X*7./2.)}{((k*X + Y/4.)*3./2. + (1-k)/2.*X*5./2.)},$$

where

$$k = \frac{(\log\rho - \log\rho_3 3)}{(\log\rho_4 - \log\rho_3)},$$

X, Y is the mass fraction of hydrogen and helium. We use the value $X = 0.73$, $Y = 0.25$. When every time the time steps are proceeded, the result of calculation for the heat energy is discarded and is replaced the pressure which are determined from the calculated value of the density. This part is the weak point of our calculation and we are now carrying out improvements.

3 Result of Calculation

In the following, we show a numerical result of our calculation for a typical model. In a simulation box with the edge length of $2\,\mathrm{AU}$, we put $T = 10\,\mathrm{K}$ isothermal spherical gas in gravitational equilibrium, and multiply the density by the factor 1.1. As a result, the mass of $1.17\,\mathrm{M}$. is contained in this simulation box. We give the gas solid rotation of the angular velocity $\Omega = 2 \times 10^2/\,\mathrm{y}$.

The grids system is such that $2^6 \times 2^6 \times 2^6$ grid cells are 20 times nested. We use the CPU Xeon on E5450 motherboard at 3.0 GHz. We have continued this calculation 3 days.

The Figure 2 show the evolution of the density at center after the time $t = 1.0155 \times 10^5\,\mathrm{y}$. When the core density reaches $0.01\,\mathrm{g\,cm^{-3}}$, the core begins to bounce.

In Figure 3, we show the density distribution before and after the bounce.

In Figure 4, we show the angular momentum distribution before the time of bounce.
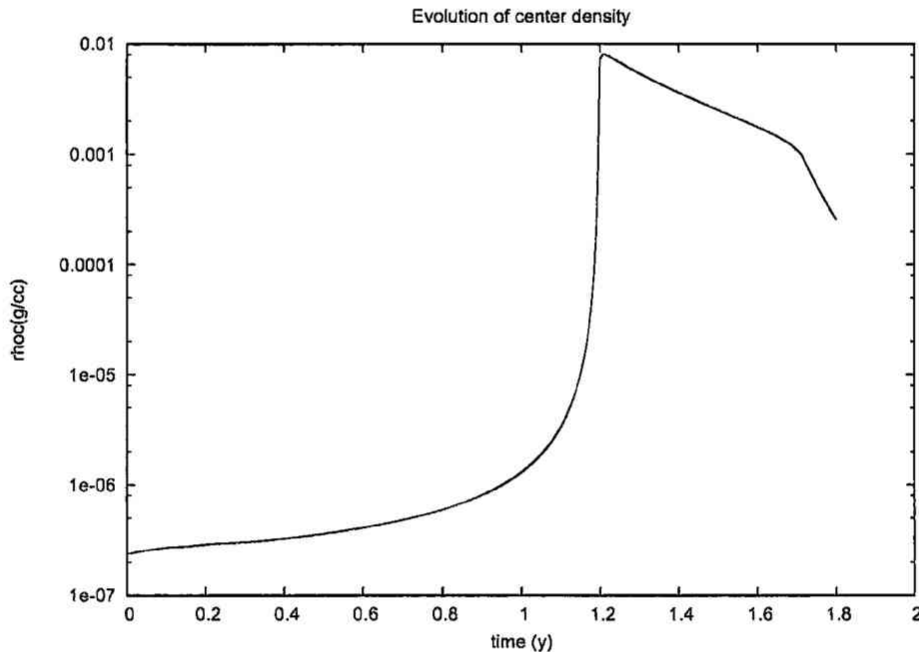

Figure 2. The density at center vs duration from $t = 1.0155 \times 10^5\,\mathrm{y}$
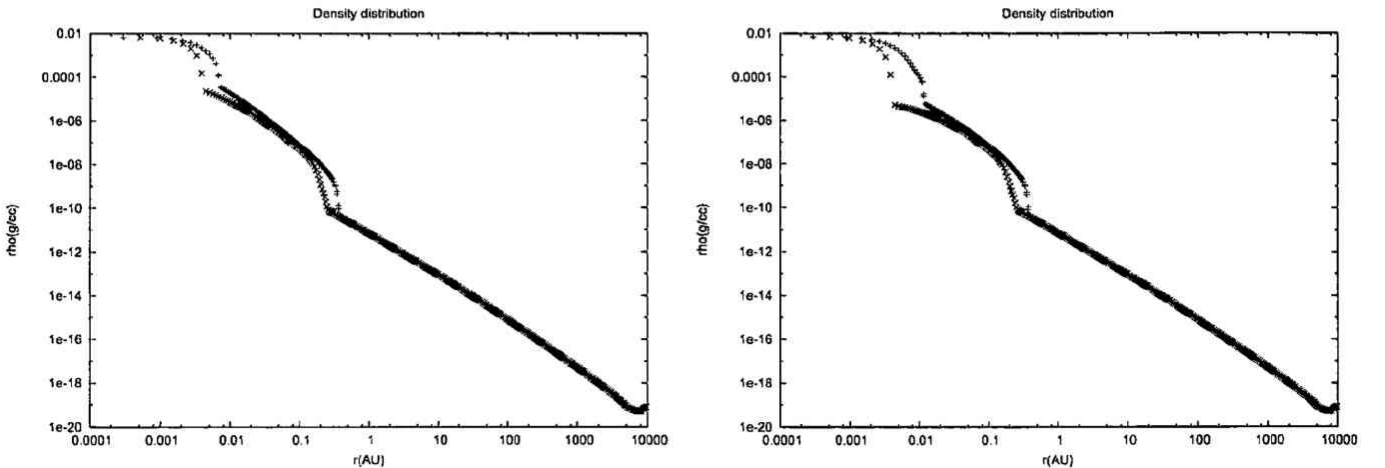

Figure 3. Density vs distance from center at $t = 1.01547546 \times 10^5\,\mathrm{y}$ (left) and $t = 1.01547558 \times 10^5\,\mathrm{y}$ (right). $+$ denote the density in the x direction, $\times$ denote ones in the z direction parallel to the rotation axis.
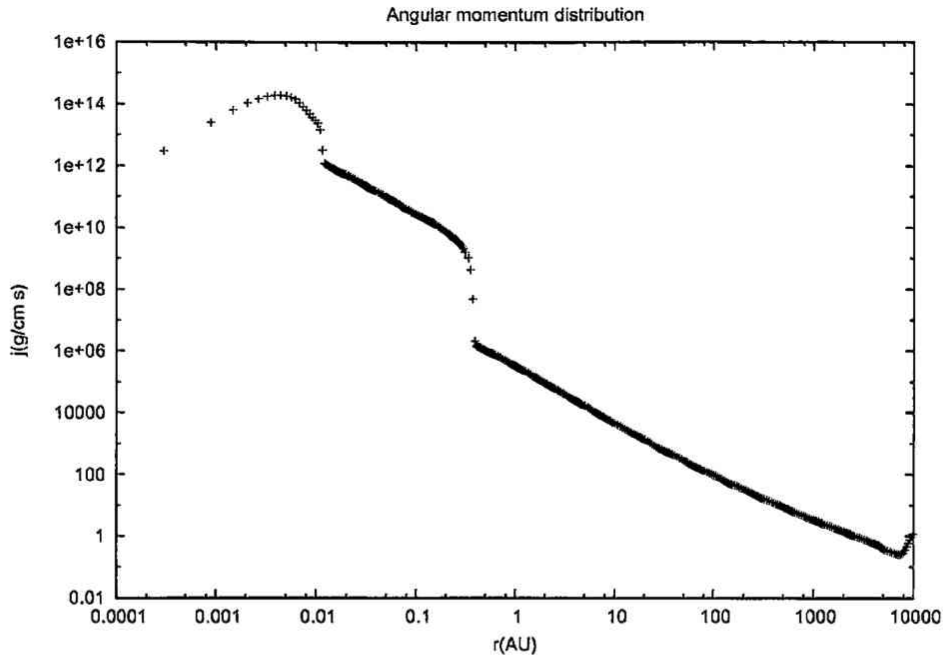
Angular momentum distribution

Figure 4. Angular momentum distribution at $t == 1.01547546 \times 10^5$ y.

4 Summary

We have constructed a code which simulates the star formation process on our personal computer. This open the possibility to study the star formation process in detail easily. We have explained the detail of the nested grids method. The point which we succeed the simulation is in the usage of the FFT to solve the Poisson equation.

References

[1] Kiguchi, M., 2002, Science and Technology, no.12, p43.

[2] Hackbusch, W., 1985, "Multi-Grid Methods and Applications", ISBN 3-540-12761-5, Springer-Verlag.

[3] Toro, E. F., 1999, "Riemann Solvers and Numerical Methods for Fluid Dynamics", ISBM 3-540-65966-8, 2nd Edition, Springer-Verlag.